Cancer Science
Japanese Cancer Association JCA
Open Access

Clinicopathological and prognostic impact of imaging of breast cancer angiogenesis and hypoxia using diffuse optical spectroscopy

Noriko Nakamiya,[1,3] Shigeto Ueda,[1,3] Takashi Shigekawa,[1] Hideki Takeuchi,[1] Hiroshi Sano,[1] Eiko Hirokawa,[1] Hiroko Shimada,[1] Hiroaki Suzuki,[2] Motoki Oda,[2] Akihiko Osaki[1] and Toshiaki Saeki[1]

[1]Department of Breast Oncology, International Medical Center, Saitama Medical University, Hidaka, Saitama; [2]Central Research Laboratory, Hamamatsu Photonics K.K., Hamamatsu-city, Japan

Key words

Angiogenesis, breast cancer, hypoxia, optical imaging, prognosis

Correspondence

Toshiaki Saeki, 1397-1 Yamane, Hidaka, Saitama 350-1298, Japan.
Tel: +81-42-984-4670 (ext. 8758); Fax: +81-42-984-4672;
E-mail: tsaeki@saitama-med.ac.jp

[3]These authors equally contributed to this work.

Funding Information

Japan Society for the Promotion of Science in Saitama Medical University (25830105). Hidaka Research Grant.

Received February 9, 2014; Revised April 18, 2014; Accepted April 23, 2014

Cancer Sci **105** (2014) 833–839

doi: 10.1111/cas.12432

Near-infrared diffuse optical spectroscopy (DOS) imaging can non-invasively measure tumor hemoglobin concentration using high contrast to normal tissue, thus providing vascularity and oxygenation status. We assessed the clinical usefulness of DOS imaging in primary breast cancer. In all, 118 women with a histologically confirmed diagnosis of primary malignant tumor were enrolled. All participants underwent testing using time-resolved DOS before treatment initiation. Visual assessment of DOS imaging for detecting tumors was carried out by two readers blinded to the clinical data. Relative total hemoglobin (rtHb) and oxygen saturation (stO_2) of the tumors was compared with clinicopathological variables and 10-year prognosis was calculated. Sensitivity for detecting a tumor based on the rtHb breast map was 62.7% (74/118). The sensitivity depended on T stage: 100% (7/7) for T3, 78.9% (45/57) for T2, 44.7% (17/38) for T1, and 31.3% (5/16) for T_{is}. Tumors showed unique features of higher rtHb with a wider range of stO_2 than normal breast tissue, depending on histological type. There was a significant correlation of rtHb with tumor size, lymphatic vascular invasion, and histological grade, and of stO_2 with age and tumor size. Neither rtHb nor stO_2 correlated with intrinsic biomarkers such as estrogen receptor, progesterone receptor, or human epidermal growth factor receptor 2; rtHb inversely correlated with 10-year relapse-free survival and overall survival, with statistical significance. Diffuse optical spectroscopy imaging has limited utility for the early detection of breast cancer; nonetheless, the findings suggest that the degree of tumor angiogenesis and hypoxia may be associated with tumor aggressiveness and poor prognosis.

Diffuse optical spectroscopy (DOS) imaging with red and near-infrared light is expected to be a next-generation modality aimed at detecting primary breast cancer. Because DOS does not use ionizing radiation or contrast agents, its clinical applications have the advantage of being safe even if the procedure is repeated in the same patient.[1] The technique can also provide biological information on tumor vascularity and oxygenation in terms of the optical properties of the tissue. The basic method involves sending a laser pulse at wavelengths of 600–1100 nm, obtaining optical signals after photons have traveled through the tissue, and finally separating absorption coefficients (μa) from reduced scattering coefficients (μs'), which are calculated from optical signals. Oxyhemoglobin (O_2Hb) and deoxyhemoglobin (HHb) are analyzed using μa, the main intrinsic absorber of breast tissue.[2] Based on the fact that the hemoglobin (Hb) concentration of breast cancer is higher than that of normal tissue, numerous studies showed that the contrast imaging could identify a tumor lesion.[3] Total Hb ($tHb = O_2Hb + HHb$) can visualize a local elevation of blood volume in a tumor, suggestive of angiogenesis; oxygen saturation ($stO_2 = O_2Hb / tHb$) reflects the degree of tumor hypoxia.[4] Pogue *et al.* reported that when comparing the features of breast tumors among patients, measuring the tHb contrast value relative to the background of normal breast tissue is more accurate than measuring the absolute value of tHb.[5]

In order to analyze the clinical utility of measuring tHb and stO_2 of a tumor lesion, we evaluated the detection rate of primary breast cancer using DOS imaging and assessed the clinicopathological and prognostic relevance of tumor tHb and stO_2.

Materials and Methods

Patient enrolment. We enrolled consecutive patients from July 2012 to April 2013 at the International Medical Center, Saitama Medical University (Saitama, Japan). After obtaining a radiological diagnosis of malignant cancer using mammography, ultrasonography (US), and/or MRI, the diagnosis was histologically confirmed in all patients using core biopsy. All patients underwent time-resolved diffuse optical spectroscopy (TRS) scans of both breasts before treatment initiation. The TRS measurements were made at least 2 weeks after the core biopsy. Clinical and histopathological information was obtained from medical

reports. The study protocol was approved by the Institutional Review Board of the International Medical Center (11-065). All patients agreed to participate in this study and signed a written informed consent form.

Data acquisition procedures. The optical properties of breast tissue were acquired using the TRS system (TRS20; Hamamatsu K.K., Hamamatsu, Japan). The functioning of the system and the procedure of data acquisition have been described elsewhere.[6] In this system, a laser source emits a laser pulse with a wavelength of 760, 800, and 834 nm, and detects temporal response profiles through tissue using the time correlate single-photon counting method.[7] On encountering the vascular regions of a tumor, the laser pulse is absorbed and scattered; this scattering is different compared with that of surrounding normal breast tissue. We obtained the tissue absorption (μa) and reduced scattering coefficients (μs') at the aforementioned wavelengths. The O_2Hb and HHb concentrations were calculated using the spectroscopic data of O_2Hb and HHb based on the photon diffusion theory.[8] A patient was tested in a supine position using a US-guided handheld probe containing a source and a detector, placed on the breast skin 3 cm apart. Measurements were taken as square or rectangular grid maps with each point separated by 10 mm in the breast. In a tumor-bearing breast, at least 49 points, which consisted of a 6 × 6 cm square grid map, were analyzed; in the contralateral normal breast, at least 25 points, which consisted of a 4 × 4 cm square grid map in a corresponding mirror image location, were analyzed. A tumor lesion as determined by US and palpation was always arrayed in the center of the map. To translate discrete data to a continuous image, we used spline interpolation, 2D image processing, and analysis. The images were 200 × 200 pixels. Visual image reconstruction was carried out using custom software (DataGridViewer, version 12; SincereTechnology Corp., Kanagawa, Japan).

A region of interest (ROI)—a circle measuring 2 cm in radius—was assigned to the skin including the area of the lesion. The number of points included in an ROI was 10–14. We set the ROI showing the highest concentration of Hb. When we could not detect a hotspot, we set the ROI just above the lesion that was identified by US. We used the mean volume calculated from ROI analysis, automatically. The evaluation of Hb parameters was carried out as follows: tHb (μM) = O_2Hb + HHb, stO_2 (%) = O_2Hb / tHb × 100, and rtHb = a ratio of tumor mean tHb to contralateral normal mean tHb. Figure 1 shows representative images of tHb and stO_2 of both tumor-bearing and contralateral normal breast.

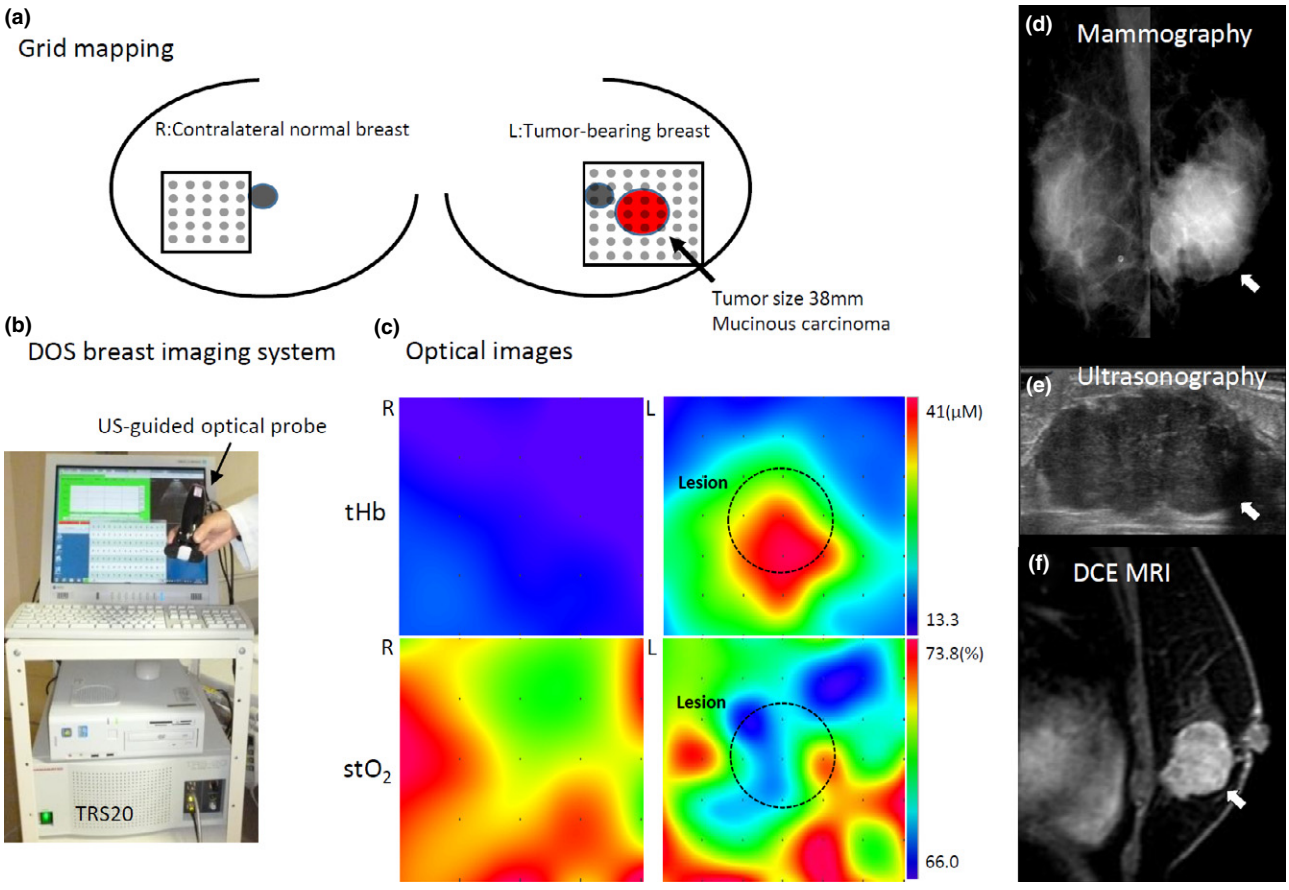

Fig. 1. Hemoglobin map construction using the optical breast imaging system. Representative images include a palpable 38-mm mucinous carcinoma on the left breast in a 56-year-old woman. (a) Optical measurements comprising a grid map over tumor (7 × 7 points, 1-cm pitch) and normal breast tissue (5 × 5 points, 1-cm pitch) are taken using a handheld probe. (b) Ultrasound (US)-guided breast imaging system with time-resolved diffuse optical spectroscopy (DOS). (c) The images present distribution of total hemoglobin (tHb) and tissue oxygen saturation (stO_2) concentrations on both breasts. (d) A mediolateral oblique mammogram shows a round circumscribed mass (arrowhead) in the subareolar area. (e) A sagittal US image obtained at the 4 o'clock position in the left breast shows a lobulated hypoechoic shadowing mass (arrowhead). (f) Dynamic contrast-enhanced (DCE) MRI shows a solitary intensely enhancing mass (arrowhead) in the lower outer quadrant of the left breast. L, left; R, right.

Interpretation of optical breast images. Two readers (N.N. and S.U.) independently evaluated the optical images of tHb in both breasts; the readers were blinded to the patients' past history and clinical and histopathological findings. When there was a discrepancy between the two readers, we discussed the case and determined the finding together. The images of tHb visualized by TRS are likely to be caused by angiogenesis in a tumor, relative to surrounding normal tissue. The most common appearance indicating tumor angiogenesis included the elevation of tumor tHb compared with normal tHb distribution or the appearance of a hotspot. Other images, which showed equivocal results, were interpreted as a uniform appearance. The definition of details has been previously described.[6] Each reader interpreted the patterns of tumor tHb distribution as either a hotspot or uniform. The hotspot tumors were considered a positive result.

Staging of primary tumors. The clinical T stage describes the tumor size and spread to the skin or to the chest wall inside the breast using MRI. In the present study, the T stage was defined as follows: T_{is}, carcinoma *in situ*; T1, tumor size ≤2 cm; T2, tumor 2–5 cm; T3, tumor size >5 cm.

Immunohistochemistry. The expressions of estrogen receptor (ER), progesterone receptor (PgR), and human epidermal growth factor receptor 2 (HER2) were examined immunohistochemically for all specimens. A monoclonal anti-ER antibody (clone ID5; 1:100), a monoclonal anti-PgR antibody (clone PgR636; 1:100), and the Herceptest kit for HER2 were purchased from Dako (Glostrup, Denmark) and used for immunohistochemical analysis. In brief, 4-μm-thick sections were deparaffinized in xylene, and dehydrated in a graded ethanol series. Antigen retrieval was carried out by the incubation of the tissue sections in a microwave oven in 10 mM sodium citrate (pH 6.0) with 0.1% Tween 40 at 120°C for 45 min. Subsequently, the tissue sections were incubated in 0.3% hydrogen peroxide in methanol for 30 min, reacted with the primary antibody for 1–3 h, incubated with a dextran polymer reagent conjugated with peroxidase and a secondary antibody (EnVision; Dako) for 1 h, and finally reacted with 3,3-diaminobenzidine tetrahydrochloride hydrogen peroxide as a chromogen. In the present study, a hormone receptor status score of 3+/2+ (≥10% nuclear staining) was regarded as positive, whereas any lower score (1+/0; <10%) was regarded as negative. Cases with a score of 3+ were considered to overexpress HER2. If a score was 2+, FISH was carried out. When the amplification of the *HER2* gene using FISH was detected, it was considered a positive result. Other situations were considered a negative result.[9]

Scoring of the Ki67 labeling index. Immunohistochemically, the Ki67 (MIB1; Dako) labeling index was measured to evaluate the proliferative activity of cancer cells. The Ki67 labeling index was counted for a minimum of 500 cancer cells from three randomly selected high-power fields containing the representative sections of the tumors. The value was calculated as a percentage of cells showing moderate to high staining intensity relative to the total number of cells. The score of ≥20% was regarded as positive, and lower scores were regarded as negative.[10]

Table 1. Sensitivity of total hemoglobin imaging for detecting primary breast tumor

T stage	No. of cases	No. of positive cases	Sensitivity, %
T_{is}	16	5	31.3
T1	38	17	44.7
T2	57	45	78.9
T3	7	7	100.0
Total	118	74	62.7

Tis, carcinoma *in situ*.

Scoring system for histological grade. A histological grade was given by two pathologists according to General Rules for Clinical and Pathological Recording of Breast Cancer, 15th edition.[11] The grade was the sum (3–9) of the nuclear pleomorphism, tubule formation, and mitotic counts scores. Nuclear pleomorphism was scored as follows: 1, small regular uniform cells; 2, moderate nuclear size and variation; and 3, marked nuclear variation. Tubular formation was scored as follows: 1, majority; 2, moderate; and 3, little or none. The mitotic count score was scored as follows: 1, 0–4 mitoses; 2, 5–10 mitoses; and 3, >10 mitoses per 10 high power fields using eyepieces of 20-mm field of view (40× objective). As shown in Table 2, a score of 3–5 was considered low grade, a score of 6–9 was considered high grade.

Measurement of glycolytic activity. In this assay of tumors, a maximum standardized uptake value (SUV_{max}) of a tumor was obtained for patients who underwent ^{18}F-fluorodeoxyglucose (FDG) PET/computed tomography (CT). Biograph 6 Hi-Rez (Siemens Medical Systems, Washington, DC, USA) was used to carry out the assay. The measurement procedure of tumor SUV_{max} was described previously in detail.[6,12] Patients fasted for at least 6 h before the ^{18}F-FDG PET/CT analysis. One hour after the i.v. administration of 3.7 Mbq/kg ^{18}F-FDG, a transmission scan using CT for attenuation correction and anatomical imaging was acquired for 90 s. The PET data were reconstructed using a combination of Fourier rebinning and the ordered-subset expectation maximization at iteration number 3 and subset 8 with attenuation correction based on CT data. An ROI was assigned to the primary lesion, including the highest uptake area (a circle of ROI, diameter 1 cm), and the SUV_{max} in ROI was calculated. The SUV was calculated according to the following formula: SUV = ROI activity (MBq/mL) / injected dose (MBq/kg of body weight).

Estimation of long-term survival. The computer program Adjuvant! Online is a tool for making decisions on adjuvant therapies for patients with breast cancer (http://www.

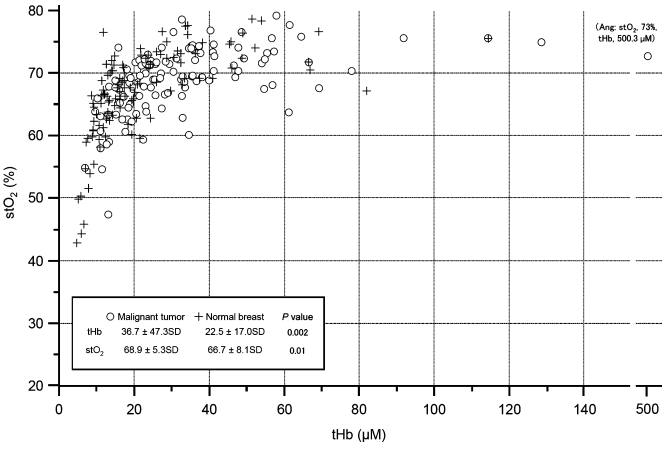

Fig. 2. Distribution of total hemoglobin (tHb) and tissue oxygen saturation (stO_2) in tumors and normal breasts. The scattergram shows distribution of absolute values of stO_2 (%) versus tHb (μM) and in tumors (blank circle) and contralateral normal breast (cross). For the contralateral normal breast, we selected a grid map in a corresponding mirror image location.

adjuvantonline.com).[13] We used this software to simulate the prognostic significance of the concentration of rtHb and stO_2 in a tumor. For the entries of information including age, menopausal status, tumor size, histological grade, degree of nodal involvement, and ER status, baseline prognostic estimates were given by each patient. The physical condition of all patients was set to average for the corresponding age. An estimated incidence of 10-year relapse-free survival and overall survival after surgical therapy was calculated by this program.[12]

Statistical analyses. All statistical analyses were carried out using MedCal software (Mariakerke, Belgium). Unpaired Student's *t*-test was used to compare variables between the two groups. Pearson's correlation analysis was used to determine a significant relationship between continuous variables and Hb parameters. Differences with a *P*-value of <5% were considered statistically significant. Values are expressed as mean ± SD unless otherwise specified.

Results

A total of 123 women participated in this study and 118 patients received a histological diagnosis of a breast malignant tumor: 15 (12.7%) had foci with associated ductal carcinoma *in situ* (DCIS), 93 (78.8%) had invasive ductal carcinoma (IDC), two (1.7%) had invasive lobular carcinomas, one (0.8%) had lobular carcinoma *in situ*, six (5.1%) had mucinous carcinomas, and one (0.8%) had angiosarcoma. The mean age of the patients was 59.3 years (±15.7 SD). The mean tumor size was 25.7 mm (±13.1 SD). The five patients who did not have fibroadenoma or any other benign tumors were assigned to the group of normal breasts. They all were diagnosed with fibrocystic disease. We set a grid map comprising 5 × 5 points with a total of 25 points in the *x*–*y* dimension in the upper outside quadrant region.

Table 2. Correlation of binary clinicopathological variables with hemoglobin parameters

		rtHb			Tumor stO2		
Variables	No.	Mean	SD	*P*-value	Mean	SD	*P*-value
Histological grade							
High	23	1.9	1.0	0.005	69.8	4.6	n.s.
Low	58	1.4	0.5		68.4	5.4	
Lymphatic vascular invasion							
Positive	22	1.9	1.1	0.020	70.8	4.7	n.s.
Negative	68	1.5	0.6		68.4	5.2	
Nodal involvement							
Positive	30	1.8	0.9	n.s.	68.8	5.2	n.s.
Negative	88	1.6	1.1		68.9	5.4	
ER status							
Positive	90	1.6	1.1	n.s	69.3	4.6	n.s.
Negative	20	1.9	1.0		68.4	6.9	
PgR status							
Positive	67	1.7	1.2	n.s.	69.4	5.0	n.s.
Negative	43	1.7	0.8		69.5	3.9	
HER2 status							
Positive	10	1.5	0.5	n.s.	69.4	5.6	n.s.
Negative	94	1.7	1.1		69.5	4.6	
Ki67 index							
High	65	1.7	1.3	n.s.	69.8	4.8	n.s.
Low	44	1.6	0.7		69.3	4.3	

ER, estrogen receptor; HER2, human epidermal growth factor receptor 2; n.s., not significant; PgR, progesterone receptor; rtHb, relative total hemoglobin; stO_2, tissue oxygen saturation.

The overall detection rate of breast tumors using DOS imaging was not impressive: 62.7% (74 of 118). Sensitivity for detecting primary tumors stratified by T stage was higher with

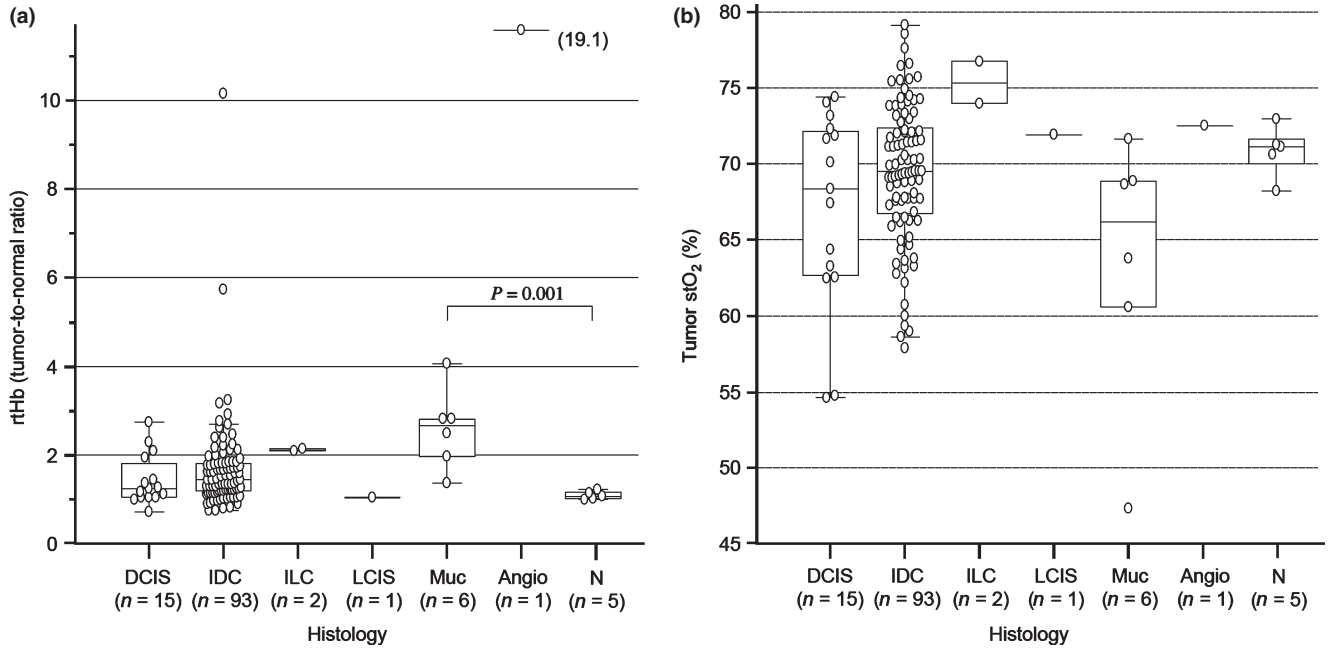

Fig. 3. (a) Relation of histological findings and degree of relative hemoglobin (rtHb). A significantly higher mean rtHb value is observed in mucinous carcinoma (Muc; 2.8 ± 0.8 SD) than in normal breast rtHb (N; 1.1 ± 0.1 SD, $P = 0.001$). Mean rtHb was not significantly different between normal breasts and other histological types, ductal carcinoma *in situ* (DCIS; 1.4 ± 0.6 SD, $P = 0.3$) and invasive ductal carcinoma (IDC; 1.7 ± 1.1 SD, $P = 0.2$). Invasive lobular carcinoma (ILC) had relatively higher rtHb (2.1) whereas lobular carcinoma *in situ* (LCIS) had low rtHb (1.1) compared to a normal breast. Angiosarcoma (Angio) showed remarkably high rtHb (19.1). (b) Relationship of histological findings and degree of tumor tissue oxygen saturation (stO_2). There were no significant differences in mean stO_2 values between normal breast (N; 70.8 ± 1.7% SD) and other histological types, DCIS (66.2 ± 6.6% SD, $P = 0.1$), IDC (69.5 ± 4.5% SD, $P = 0.5$), and mucinous carcinoma (Muc; 61.8 ± 8.8% SD, $P = 0.06$).

a more advanced T-stage as follows: T_{is}, 31.3% (5 of 16); T1, 44.7% (17 of 38); T2, 78.9% (45 of 57); and T3, 100% (7 of 7; Table 1).

Figure 2 shows a scattergraph of stO_2 versus tHb. Malignant tumors showed significantly higher tHb and higher stO_2 than did a contralateral normal breast.

Figure 3(a) shows rtHb levels. In normal breast tissue, mean rtHb was 1.09 ± 0.1 SD. Compared with normal breast tissue, only mucinous carcinoma showed a significantly higher rtHb level, but there were no significant differences between normal breasts and other histological types. Figure 3(b) shows the mean stO_2 of a normal breast ($70.8\% \pm 1.7\%$ SD) and a wide range of stO_2 of malignant tumors ($69\% \pm 5.3\%$ SD).

As shown in Table 2, which compares the values of Hb parameters with the binary classification of clinicopathological variables, tumors with a higher grade and positive for lymphatic vascular invasion (LVI) had significantly higher rtHb level than those of lower grade and negative for LVI. There was no significant association between tumor stO_2 and clinicopathological variables.

Table 3 shows correlation coefficients and *P*-values when clinical continuous variables and Hb parameters were compared. Relative total hemoglobin positively correlated with tumor size and grade, whereas tumor stO_2 inversely correlated with age and positively correlated with tumor size, with statistical significance. Higher rtHb of a tumor indicated a significantly higher glycolytic activity (measured as FDG−SUV_{max}) and possibly poorer 10-year relapse-free survival and overall survival.

Discussion

In the light of the visual assessment of the tHb breast map, 74 (62.7%) tumors were detected in 118 patients with primary malignant tumors. Sensitivity for detecting early breast tumors was low (T_{is}, 31.3%; T1, 44.7%) in our approach. Some studies using US-guided DOS imaging similar to ours revealed a sensitivity of 75–92% and specificity of 67–93% in distinguishing breast cancer from benign tumors.[14,15] However, these studies consisted only of tumors that were already identified using US. This approach does not appear to be helpful in cancer screening.

Figure 2 shows that a malignant tumor shows an increased absolute value of tHb and is shifted to the right compared to normal breasts, while maintaining high stO_2. It is reasonable to interpret this result as follows: malignant tumors induce angiogenesis due to sustained tissue oxygenation.[16] Therefore, we can hypothesize that rtHb, or tumor/background ratio of tHb, might be an indicator of the degree of tumor angiogenesis. The finding of a positive correlation of rtHb and histopathological characteristics, such as histological grade and LVI status (Tables 2 and 3), supports the notion that rtHb is a biomarker of aggressiveness.

There was a significant correlation of rtHb with tumor glycolytic activity measured using FDG-PET/CT ($r = 0.45$, $P < 0.0001$),

Table 3. Correlation of continuous variables with hemoglobin parameters

	Values	rtHb		stO2	
		Correlation coefficient *r*	*P*-value	Correlation coefficient *r*	*P*-value
A. Clinicopathology					
Age					
No.	118	0.17	n.s.	−0.25	0.005
Mean, years	59.3				
SD	13.1				
Tumor size					
No.	118	0.28	0.0020	0.20	0.040
Mean, mm	25.7				
SD	15.7				
Histological grade					
No.	81	0.30	0.0080	0.15	n.s.
Mean	5.9				
SD	1.4				
B. Metabolism					
Glycolytic activity (FDG−SUV_{max})					
No.	70	0.48	<0.0001	0.02	n.s.
Mean	4.9				
SD	3.7				
C. Prognosis					
10-year relapse-free survival					
No.	98	−0.22	0.0300	0.14	n.s.
Mean, %	50.5				
SD	19.5				
10-year overall survival					
No.	98	−0.22	0.0300	0.17	n.s.
Mean, %	65.8				
SD	20.7				

FDG, ^{18}F-fluoro-deoxy-glucose; n.s., not significant; rtHb, relative total hemoglobin; SD, standard deviation; stO_2, tissue oxygen saturation; SUV, standardized uptake value.

without any association with the molecular biomarkers ER, PgR, or HER2. This finding suggests that rtHb depends more on physiological status rather than an intrinsic subtype based on molecular biological findings.[17]

Different Hb characteristics of different histological types gave us some idea about angiogenesis and hypoxia in these tumors (Fig. 3). Ductal carcinoma *in situ* refers to a heterogeneous group of tumors with a variety of vascular patterns.[18] In this study, the rtHb level did not significantly differ between DCIS tumors and normal breast tissue. Lower rtHb level in DCIS tumors was probably because of the smaller density of angiogenesis in DCIS than in invasive cancer.[19,20] Our findings revealed a high rtHb level along with a wide range of stO_2 for IDC, which was probably related to the higher degree of angiogenesis and hypoxia found in the tumor. We previously reported that tumors with a pathologic complete response to neoadjuvant chemotherapy have significantly higher tumor stO_2 than those without pathologic complete response.[21] Thus, the degree of tumor hypoxia could be a significant biomarker to predict chemosensitivity. In our present results, mucinous carcinoma shows unique characteristics of a remarkably higher rtHb level along with stO_2 lower than in the other histological types. Mucinous carcinoma is characterized by rim enhancement with a persistent enhanced pattern with a rich mucin pool at the center of a tumor on dynamic MRI imaging[22] and a poor response to chemotherapy.[23] These pathological characteristics could be in agreement with the Hb features of mucinous carcinoma.

Angiosarcoma is a rare and highly malignant soft-tissue sarcoma of endovascular origin with a poor overall prognosis.[24] Dynamic MRI revealed heterogeneous appearance with markedly rich vascularity and hemorrhage.[25] Imaging revealed an angiosarcoma harboring >10-fold higher mean rtHb (mean, 19.1) than that of IDC (mean, 1.5).

Considering the positive correlation of rtHb and prognostic variables such as tumor size, grade, and LVI, we can hypothesize that a patient group with a higher rtHb level might have poorer prognosis (Table 3). The degree of angiogenesis reportedly has prognostic utility in primary breast cancer.[26,27] A follow-up study on these patients is needed to confirm this result.

There are several possible limitations to our study with respect to the optical assessment of breast cancer. Low spatial resolution of DOS with intrinsic natural contrast results in difficulty in interpreting high-contrast tumor images in comparison with surrounding normal tissue.[28] The underlying thoracic muscle of the breast might cause substantial image artifacts because the Hb- and myoglobin-rich muscles are intense absorbers.[29] A peak tHb value was not always identical to the center of a tumor lesion identified by US. The peak appeared to shift slightly to areola, sternum, or axilla region of the breast, depending on individual tumor locations. This inaccuracy might result in an erroneous interpretation of imaging data.

In conclusion, vascular and hypoxia imaging obtained with DOS are a new intriguing topic with demonstrated implications for the functional diagnosis of breast cancer. Although DOS imaging is not suitable for early diagnosis of breast cancer, Hb parameters could stratify the unique features of tumor angiogenesis in relation to hypoxia, which may affect tumor aggressiveness and patients' prognosis.

Acknowledgments

The authors thank Noriko Wakui for her excellent technical assistance and Yukio Ueda, PhD and Yutaka Yamashita, Central Research Laboratory, Hamamatsu Photonics K.K. for their sincere cooperation in this research. This work was supported by the Japan Society for the Promotion of Science, Kakenhi (Grant No. 25830105) and a Hidaka Research Grant.

Disclosure Statement

The authors have no conflict of interest.

References

1 Tromberg BJ, Pogue BW, Paulsen KD, Yodh AG, Boas DA, Cerussi AE. Assessing the future of diffuse optical imaging technologies for breast cancer management. *Med Phys* 2008; **35**: 2443–51.
2 Ueda Y, Yoshimoto K, Ohmae E *et al.* Time-resolved optical mammography and its preliminary clinical results. *Technol Cancer Res Treat* 2011; **10**: 393–401.
3 Massimiliano D, Giuseppe F, Maria L, Adolfo G, *et al.* The dynamic optical breast imaging in the preoperative workflow of women with suspicious or malignant breast lesions: development of a new comprehensive score. *ISRN Oncol* 2012; **2012**: article ID 631917, 9 pages.
4 Tromberg BJ, Cerussi A, Shah N *et al.* Imaging in breast cancer: diffuse optics in breast cancer: detecting tumors in pre-menopausal women and monitoring neoadjuvant chemotherapy. *Breast Cancer Res* 2005; **7**: 279–85.
5 Pogue BW, Jiang S, Dehghani H *et al.* Characterization of hemoglobin, water, and NIR scattering in breast tissue: analysis of intersubject variability and menstrual cycle changes. *J Biomed Opt* 2004; **9**: 541–52.
6 Ueda S, Nakamiya N, Matsuura K *et al.* Optical imaging of tumor vascularity associated with proliferation and glucose metabolism in early breast cancer: clinical application of total hemoglobin measurements in the breast. *BMC Cancer* 2013; **13**: 514.
7 Ohmae E, Ouchi Y, Oda M *et al.* Cerebral hemodynamics evaluation by near-infrared time-resolved spectroscopy: correlation with simultaneous positron emission tomography measurements. *Neuroimage* 2006; **29**: 697–705.
8 Patterson MS, Chance B, Wilson BC. Time resolved reflectance and transmittance for the non-invasive measurement of tissue optical properties. *Appl Opt* 1989; **28**: 2331–6.
9 Ueda S, Tsuda H, Sato K *et al.* Alternative tyrosine phosphorylation of signaling kinases according to hormone receptor status in breast cancer overexpressing the insulin-like growth factor receptor type 1. *Cancer Sci* 2006; **97**: 597–604.
10 Ueda S, Tsuda H, Saeki T *et al.* Early metabolic response to neoadjuvant letrozole, measured by FDG PET/CT, is correlated with a decrease in the Ki67 labeling index in patients with hormone receptor-positive primary breast cancer: a pilot study. *Breast Cancer* 2011; **18**: 299–308.
11 Sakamoto G, Inaji H, Akiyama F, *et al.* General rules for clinical and pathological recording of breast cancer 2005. *Breast Cancer* 2005; **12**(Suppl): S1–27.
12 Ueda S, Tsuda H, Asakawa H *et al.* Clinicopathological and prognostic relevance of uptake level using 18F-fluorodeoxyglucose positron emission tomography/computed tomography fusion imaging (18F-FDG PET/CT) in primary breast cancer. *Jpn J Clin Oncol* 2008; **38**: 250–8.
13 Ravdin PM, Siminoff LA, Davis GJ *et al.* Computer program to assist in making decisions about adjuvant therapy for women with early breast cancer. *J Clin Oncol* 2001; **19**: 980–91.
14 You SS, Jiang YX, Zhu QL, Liu JB, Zhang J, Dai Q *et al.* US-guided diffused optical tomography: a promising functional imaging technique in breast lesions. *Eur Radiol* 2010; **20**: 309–17.
15 Zhu Q, Hegde PU, Ricci A Jr *et al.* Early-stage invasive breast cancers: potential role of optical tomography with US localization in assisting diagnosis. *Radiology* 2010; **256**: 367–78.
16 Folkman J. Tumor angiogenesis: therapeutic implications. *N Engl J Med* 1971; **285**: 1182–6.
17 Sorlie T, Perou CM, Tibshirani R *et al.* Gene expression patterns of breast carcinomas distinguish tumor subclasses with clinical implications. *Proc Natl Acad Sci USA* 2001; **98**: 10869–74.

18 Yamada T, Mori N, Watanabe M, *et al.* Radiologic-pathologic correlation of ductal carcinoma in situ. *Radiographics* 2010; **30**: 1183–98.
19 Adler EH, Sunkara JL, Patchefsky AS, Koss LG, Oktay MH. Predictors of disease progression in ductal carcinoma in situ of the breast and vascular patterns. *Hum Pathol* 2012; **43**: 550–6.
20 Teo NB, Shoker BS, Jarvis C, Martin L, Sloane JP, Holcombe C. Vascular density and phenotype around ductal carcinoma in situ (DCIS) of the breast. *Br J Cancer* 2002; **86**: 905–11.
21 Ueda S, Roblyer D, Cerussi A *et al.* Baseline tumor oxygen saturation correlates with a pathologic complete response in breast cancer patients undergoing neoadjuvant chemotherapy. *Cancer Res* 2012; **72**: 4318–28.
22 Monzawa S, Yokokawa M, Sakuma T *et al.* Mucinous carcinoma of the breast: MRI features of pure and mixed forms with histopathologic correlation. *AJR Am J Roentgenol* 2009; **192**: W125–31.
23 Nagao T, Kinoshita T, Hojo T, Tsuda H, Tamura K, Fujiwara Y. The differences in the histological types of breast cancer and the response to neoadjuvant chemotherapy: the relationship between the outcome and the clinicopathological characteristics. *Breast* 2012; **21**: 289–95.
24 Buatti JM, Harari PM, Leigh BR, Cassady JR. Radiation-induced angiosarcoma of the breast. Case report and review of the literature. *Am J Clin Oncol* 1994; **17**: 444–7.
25 Yang WT, Hennessy BT, Dryden MJ, Valero V, Hunt KK, Krishnamurthy S. Mammary angiosarcomas: imaging findings in 24 patients. *Radiology* 2007; **242**: 725–34.
26 Arnes JB, Stefansson IM, Straume O *et al.* Vascular proliferation is a prognostic factor in breast cancer. *Breast Cancer Res Treat* 2012; **133**: 501–10.
27 Gluz O, Wild P, Liedtke C *et al.* Tumor angiogenesis as prognostic and predictive marker for chemotherapy dose-intensification efficacy in high-risk breast cancer patients within the WSG AM-01 trial. *Breast Cancer Res Treat* 2011; **126**: 643–51.
28 Yang WT. Emerging techniques and molecular imaging in breast cancer. *Semin Ultrasound CT MR* 2011; **32**: 288–99.
29 Ardeshirpour Y, Huang M, Zhu Q. Effect of the chest wall on breast lesion reconstruction. *J Biomed Opt* 2009; **14**: 044005.